

* . * . **

A Fundamental Study of the Supersonic Coherent Jet

Mi-Seon Jeong, Wee-Bun Cho and Heuy-Dong Kim

Key Words : Compressible Flow(), Combustion(), Supersonic Jet(),
Supersonic Coherent Jet(), Correctly-Expanded Jet(),
Jet Core Length()

Abstract

In steel-making processes of iron and steel industry, the purity and quality of steel can be dependent on the amount of CO contained in the molten metal. Recently, the supersonic oxygen jet is being applied to the molten metal in the electric furnace and thus reduces the CO amount through the chemical reactions between the oxygen jet and molten metal, leading to a better quality of steel. In this application, the supersonic oxygen jet is limited in the distance over which the supersonic velocity is maintained. In order to get longer supersonic jet propagation into the molten metal, a supersonic coherent jet is suggested as one of the alternatives which are applicable to the electric furnace system. It has a flame around the conventional supersonic jet and thus the entrainment effect of the surrounding gas into the supersonic jet is reduced, leading to a longer propagation of the supersonic jet. The objective of the present study is to investigate the supersonic coherent jet flow. A computational study is carried out to solve the compressible, axisymmetric Navier-Stokes equations. The computational results of the supersonic coherent jet are compared with the conventional supersonic jet.

1. 가 ,
가 ,
3-5% (1-4).
가 ,
가 ,
가 가
(entrainment)
가 ,
가

**

E-mail : kimhd@andong.ac.kr
TEL : (054)820-5622 FAX : (054)823-5495

*

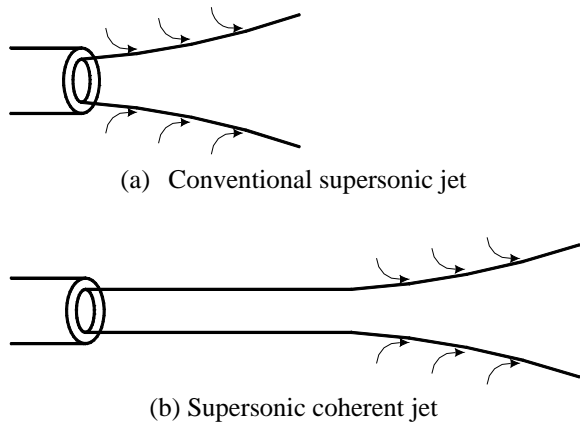


Fig. 1 Schematics of a conventional supersonic jet and a supersonic coherent jet

$$\frac{\partial \rho}{\partial t} + \frac{\partial}{\partial x_i} (\rho u_i) = 0 \tag{1}$$

$$\frac{\partial}{\partial t} (\rho u_i) + \frac{\partial}{\partial x_j} (\rho u_i u_j) = \frac{\partial}{\partial x_j} \left[\mu \left(\frac{\partial u_i}{\partial x_j} + \frac{\partial u_j}{\partial x_i} \right) \right] \tag{2}$$

$$- \frac{\partial}{\partial x_i} \left(\frac{2}{3} \mu \frac{\partial u_i}{\partial x_i} \right) - \frac{\partial p}{\partial x_i} + \frac{\partial}{\partial x_j} \left(- \rho u_i u_j \right)$$

$$\frac{\partial}{\partial t} (\rho E) + \frac{\partial}{\partial x_i} (\rho u_i H) =$$

$$\frac{\partial}{\partial x_j} \left[\left(x + \frac{\mu_t}{Pr_t} \right) \frac{\partial T}{\partial x_i} + u_j (\tau_{ij})_{eff} \right] \tag{3}$$

Fig.1 가
 coherent Fig.1 (a) 가
 Fig.1 (b) coherent 가
 coherent Mathur
 coherent Brhel⁽⁹⁾
 coherent
 coherent
 coherent
 coherent 가
 Navier-Stokes
 k-ε
 2.
 coherent
 k-ε
 Navier-Stokes

4 Runge-Kutta

(Probability Density Function)
(11-12)

$$\frac{\partial}{\partial t} (\rho \bar{f}) + \frac{\partial}{\partial x_i} (\rho u_i \bar{f}) = \frac{\partial}{\partial x_i} \left(\frac{\mu_t}{\sigma_t} \frac{\partial \bar{f}}{\partial x_i} \right) \tag{4}$$

$$\frac{\partial}{\partial t} (\rho \overline{f'^2}) + \frac{\partial}{\partial x_i} (\rho u_i \overline{f'^2}) =$$

$$\frac{\partial}{\partial x_i} \left(\frac{\mu_t}{\sigma_t} \frac{\partial \overline{f'^2}}{\partial x_i} \right) + C_g \mu_t \left(\frac{\partial \bar{f}}{\partial x_i} \right)^2 - C_d \rho \frac{\epsilon}{k} \overline{f'^2} \tag{5}$$

f (mixture fraction)

$$f = \frac{Z_i - Z_{i,ox}}{Z_{i,fuel} - Z_{i,ox}}$$

Z_i i
 ox fuel
 σ_t C_g C_d

0.7, 2.86, 2.0 (12)

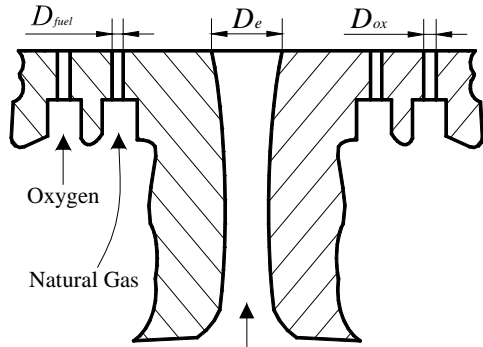
$$(5) \rho u_i' \overline{f'}$$

$$\rho u_i' \overline{f'} = - \frac{\mu_t}{\sigma_t} \frac{\partial \bar{f}}{\partial x_i} \tag{6}$$

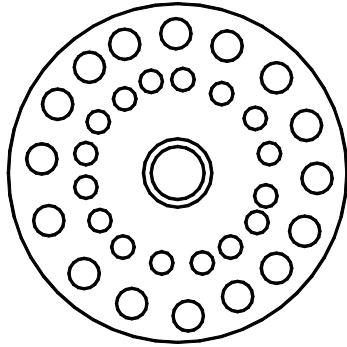
$$\bar{\phi} = \int_0^1 \phi(f) p(f) df \tag{7}$$

CH₄ , O₂

Natural gas



(a) Coherent nozzle



(b) Cross-sectional nozzle used in experiments

Fig. 2 Schematics of the supersonic coherent nozzle

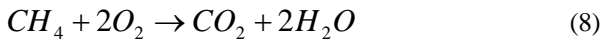


Fig. 2

Fig. 2 (a) (10)

(throat) 0.427inch $(D_e) \quad 0.58\text{inch}$, 가 2.0 가 Natural gas

Oxygen 0.113inch , $D_{ox} = 0.161\text{inch}$ Fig. 2 (b) $D_{fuel} =$ (10)

2 가

Fig. 3

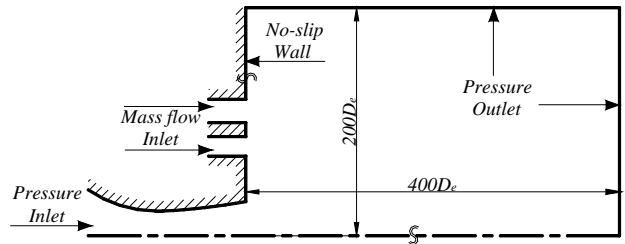
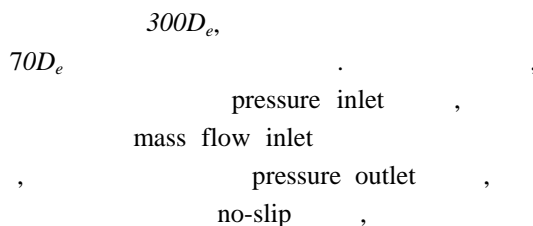


Fig. 3 Computational flow field and boundary conditions

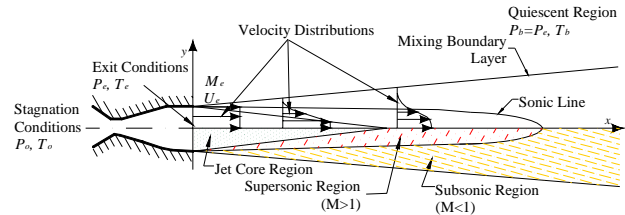


Fig. 4 Schematic of supersonic correctly-expanded jet

4

, , , $k \quad \epsilon \quad 10^{-4}$

,

0.5%

가

3.

Fig. 4

P_o, T_o , P_e, T_e , P_b, T_b

가

(sonic lone)

(jet core length)

(sonic line)

(supersonic length) (13)

Fig. 5

$M_e = 2.0, P_b/P_e = 1.0$

coherent

Fig. 5 (a)

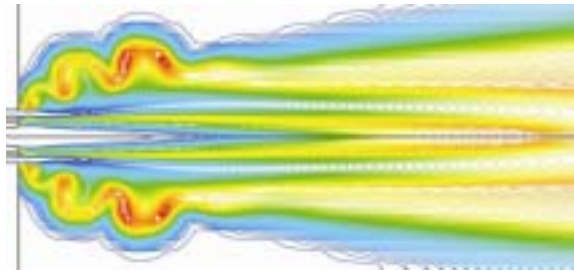
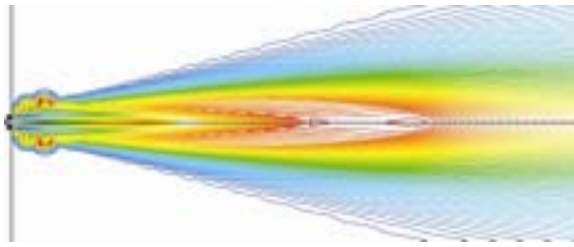


Fig. 5 Static temperature contours of the supersonic coherent jet ($M_e = 2.0, P_b/P_e = 1.0$)

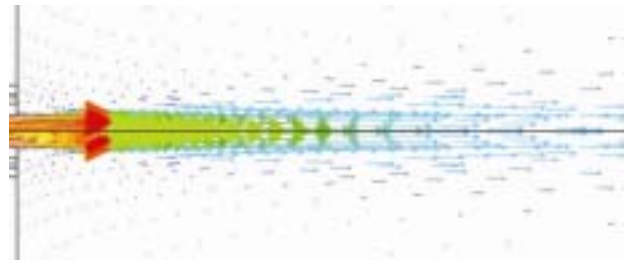


Fig. 6 Velocity vector contours ($M_e = 2.0, P_b/P_e = 1.0$)

가
 (fluctuation)
 Fig.6
 Fig.6 (a)
 Fig.6 (b)

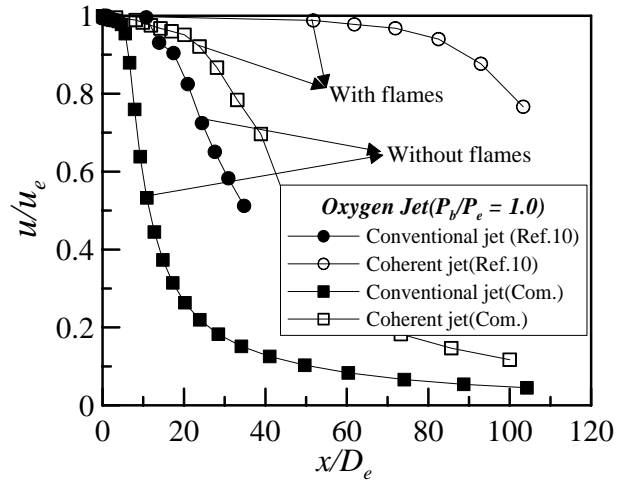
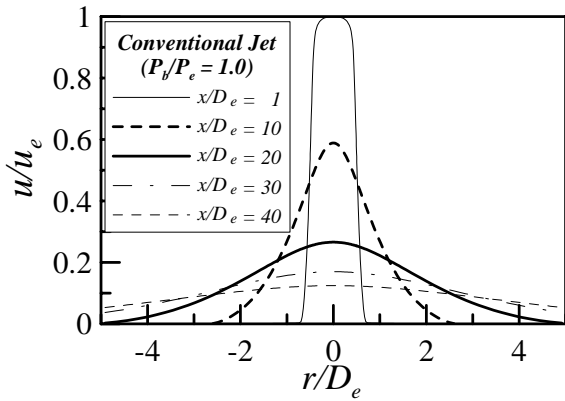


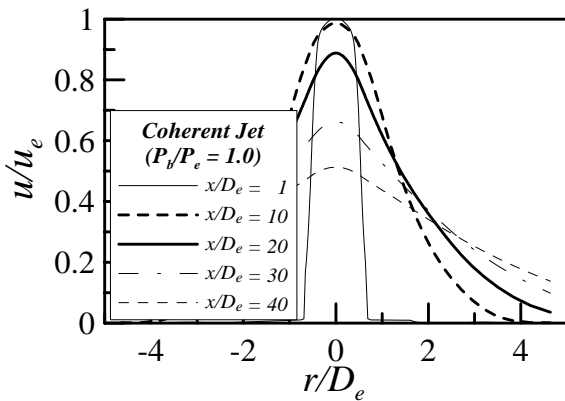
Fig. 7 Velocity distributions along the jet axis ($P_b/P_e = 1.0, M_e = 2.0$)

Fig.7
 Fig.8
 coherent
 7~8
 20 ~ 25
 3
 closed symbol (●, ■)
 open symbol (○, □)
 coherent (○, ●)
 (10)
 (□, ■)
 (Fig.2 (b))
 coherent

$x/D_e = 1, 10, 20, 30$
 Fig. 8 (a) , $x/D_e=1$
 ($r/D_e=0$)
 가, x/D_e 가 가
 , ,
 Fig. 8 (b)
 coherent
 ,
 coherent 가
 가 ,
 coherent 가
 Fig. 9 (M_e)가 2.0, (P_b/P_e)가
 1.0 coherent
 가 coherent



(a) Conventional supersonic jet



(b) Supersonic coherent jet

Fig. 8 Radial velocity distributions ($M_e = 2.0, P_b/P_e = 1.0$)

Fig. 10 가 2.0 coherent
 (P_b/P_e)
 Fig. 10 (a)
 $P_b/P_e = 0.8$

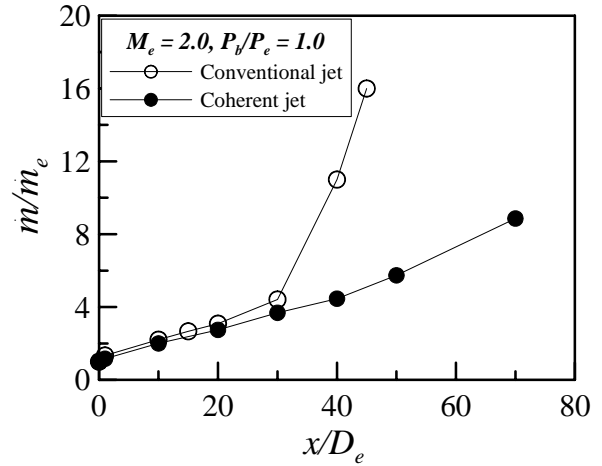


Fig. 9 Mass flow rate of the conventional jet and coherent jet ($M_e = 2.0, P_b/P_e = 1.0$)

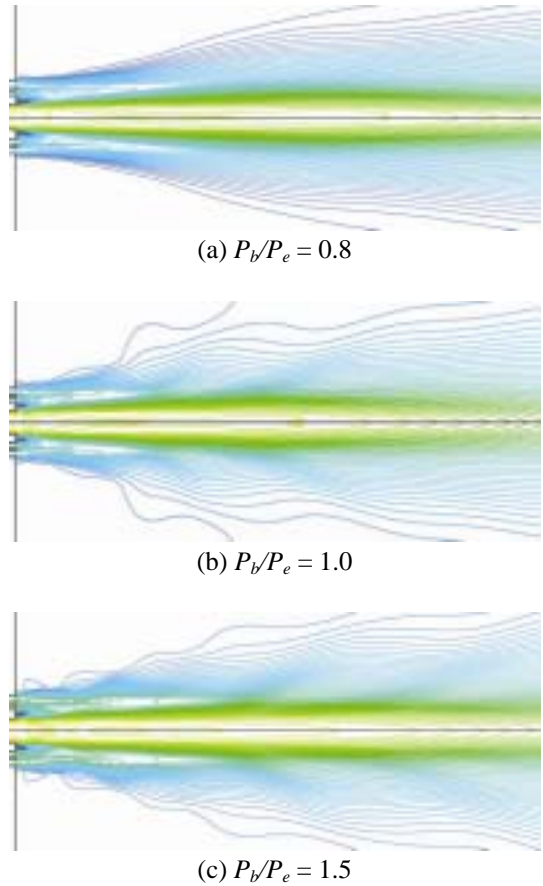


Fig. 10 Velocity contours for various pressure ratios ($M_e = 2.0$)

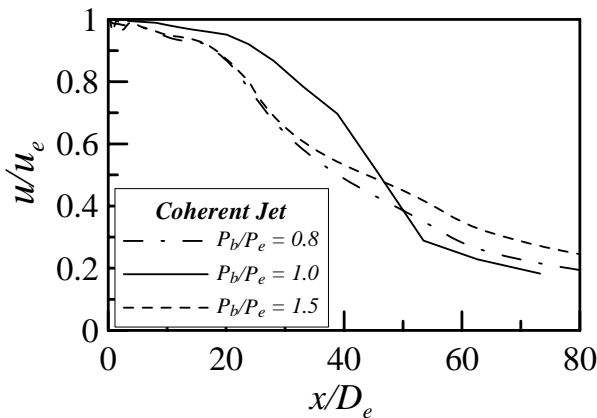


Fig. 11 Velocity distributions along the jet axis ($M_e = 2.0$)

(b) $(P_b/P_e) > 1.0$, Fig.9 (c) $(P_b/P_e) > 1.5$ Fig.10

Fig.11 coherent (P_b/P_e)

$P_b/P_e = 0.8$, $x/D_e < 45$, $P_b/P_e = 1.0$, $x/D_e > 45$

$P_b/P_e = 1.5$, $x/D_e = 30$, $P_b/P_e = 1.0$, $x/D_e < 50$, $x/D_e > 50$

4. Navier-Stokes coherent

(1) 가 coherent

(2) 3 coherent

coherent 가

(3) coherent 가 coherent

(4) 가 coherent

3

2

coherent

2003 21

- (1) Fox, J. H., 1974, "On the Structure of Jet Plumes," J. AIAA, Vol.12, pp.105-107.
- (2) Hu, T. and McLaughlin, D., 1990, "Flow and Acoustic Properties of Low Reynolds number Underexpanded Supersonic Jets," J. Sound and Vibration, Vol.141, pp.485-505.
- (3) Love, E. S., Grigsby, C. E., Lee, L. P. and Woodling, M. J., 1959, "Experimental and Theoretical Studies of Axisymmetric Free Jet," NASA TR R-6.
- (4) Amson, T. and Nicolls, J., 1959, "On the Structure of Jets from Highly Underexpanded Nozzles into still Air," J. Aero space Science, Jan., pp.16-24.
- (5) Mathur, P. C., Konicsics, D. and Engle, D., 1997, "Results of Oxygen Injection in the EAF with Praxair Coherent Jet Injectors: A Novel Technology," Electric Furnace Conference Proceedings, ISS, Vol.55, pp.305-313.
- (6) Busboom, E. Cooper, S. and Daubler, L., 1998, "Improving EAF Productivity with Praxair Coherent Jet Technology," Electric Furnace Conference, November.
- (7) Sarma, B. et al., 1998, "Fundamental Aspects of Coherent Gas Jets," Electric Furnace Conference Proceedings, ISS, Vol.56, pp.657-672.
- (8) Anderson, J. E., Mathur, P. C. and Selines, R. J., 1998, "Method and Introducing Gas into a Liquid," U.S. Patent No.5814125, September.
- (9) Brhel, J., Shver, V., Coburn, M., Blakemore R. and Mendrek, A., 2001, "An Improved Method of Applying Chemical Energy into the EAF," Air Products and Chemicals, Inc.
- (10) Anderson, J. E., Sommers, N. Y., Farrenkopf, D. R. and Bethal, Conn., 1998, "Coherent Gas Jet," U.S. Patent No.5823762, Oct.
- (11) Bish, E. S. and Norton T. S., 1998, "Numerical Modeling of Turbulent Jet Diffusion Flames: Challenges and Implications for Flare Flame Simulations," America/Japanese Flame Research Committee Int'l Symposium, October.
- (12) FLUENT V6 User's Guide, 2001, Volume 3, Fluent, Inc.
- (13) Shire, J. W. and Seubold, J. G., 1967, "Length of the Supersonic Core in High-Speed Jets," J. AIAA, Vol.5, pp.2062-2064.